

The impact of transformation plasticity on the Electron Beam welding of thick-section ferritic steel components

**Anastasia N. Vasileiou¹, Michael C. Smith², Balakrishnan Jeyaganesh¹,
John A. Francis³ and Cory J. Hamelin⁴**

¹ Post-doctoral research associate, School of MACE, The University of Manchester, UK

² Professor of Welding Technology, Director, EDF Modelling and Simulation Centre, EPSRC Manufacturing Fellow, The University of Manchester, UK

³ Senior Lecturer in Welding Technology, The University of Manchester, UK

⁴ Structural Materials Engineer, ANSTO, Institute of Materials Engineering, AU

ABSTRACT

Welding is an important process used during the construction and maintenance of nuclear reactor components. Welding results in residual stresses, distortions and microstructural changes in the joined components, which can have significant deleterious effects on their in-service performance. It is thus crucial for engineers to effectively predict these effects.

Ferritic steels undergo solid-state phase transformation (SSPT) during heating and cooling, thus making welding simulation challenging. The volumetric changes resulting from SSPT can also cause transformation-induced plasticity. The importance of transformation plasticity for single-pass, autogenous welding of a thick component is the subject of this paper.

Electron beam (EB) welding was the technique chosen to weld 30-mm thick ferritic steel plates using a single pass. The welded plates were instrumented with thermocouple arrays, to capture the far-field and near-field thermal transients on the top and bottom surfaces during the welding and the cooling down process. Welding distortions were subsequently measured using laser profilometry. Distributions of the developed residual stresses were measured using the neutron diffraction (ND) method.

Numerical finite element analysis (FEA) was used to simulate the welding process. After calibrating the thermal solution using thermocouple data, mechanical analysis was conducted using three different approaches: (i) taking account of anisothermal SSPT kinetics with transformation plasticity; (ii) taking account of anisothermal SSPT kinetics without transformation plasticity; and (iii) assuming isothermal SSPT kinetics. The predicted residual stresses and structural distortions are compared to the experimental data, thus assessing the Influence of different SSPT phenomena.

INTRODUCTION

SA508 is a ferritic, low alloy steel commonly used in nuclear components with SA508 Gr.3 being mainly used in Pressurized Water Reactors (PWR). The welding methods currently being used to weld these components are based on arc welding processes such as manual metal arc (MMA) welding, submerged arc welding (SAW) and gas tungsten arc welding (GTAW). Traditional arc welding, even in the case of narrow groove (NG) arc welding, involves multiple passes as well as the addition of filler metal. Electron beam (EB) welding, on the other hand, is autogenous and can be a single pass process. EB welding performed under vacuum is called Reduced Pressure Electron Beam (RPEB) welding, which has the advantage of no oxidation (Duffy (2014)). A single pass process can lead to significantly higher productivity, since multiple days of welding could be replaced by a several-hour long procedure.

Ferritic steels experience solid-state phase transformations (SSPTs) which cause volumetric changes due to differences in the atomic packing density of various phases in the steel (Francis, Bhadeshia, and Withers (2007)). SSPT occurs in a different way on heating as it does on cooling, due to the anisothermal nature of the transformation kinetics. Weld modelling for the prediction of weld residual stresses (WRS) has proved to be challenging due to these phenomena. Five components of strain, as proposed by Sjöström (1985), should be taken into consideration to describe SSPT:

$$\varepsilon = \varepsilon^e + \varepsilon^p + \varepsilon^{th} + \varepsilon^{tr} + \varepsilon^{tp}. \quad (1)$$

The strain components comprise the elastic strain (ε^e), the plastic strain (ε^p), the thermal strain (ε^{th}), the metallurgical transformation strain (ε^{tr}) and the transformation-induced plasticity (ε^{tp}). The last two components of strain, ε^{tr} and ε^{tp} , are created during SSPT.

Transformation plasticity (TP) can be produced via two mechanisms: the first one is numerically described by the Greenwood and Johnson model (Greenwood and Johnson (1965)), and the second one by the Magee model (Magee (1966)). Recent state-of-the-art publications in weld modelling use algorithms that consider both mechanisms. Such models are not yet extensively validated for different welding processes. It is furthermore reported that the details of any implementation of SSPT kinetics can significantly affect the accuracy of the model. However, the impact of transformation plasticity is not clearly confirmed (Hamelin et al. (2014)).

The present work focuses on comparing different modelling approaches concerning TP, using a well-characterised benchmark study: a single-pass, autogenous EB ferritic weld. WRS results are compared with experimental data from neutron diffraction (ND) measurements.

EXPERIMENT

Base Materials and Design of welding specimens

The base material consisted of SA508 ferritic steel, Grade 3, Class 1, having the chemical composition shown in Table 1. The dimensions of the final welded plates were 300 x 200 x 30 mm. Square edge grooves were machined from each plate to produce square-butt welds. The weld preparation drawings for 30-mm thick plates are shown in Figure 1.

Table 1: Nominal composition of SA508 Grade 3 Class 1 steel (wt.%).

C	Si	Cr	Co	Mn	Ni	Mo	Fe
0.16	0.27	0.23	0.004	1.43	0.77	0.52	Bal.

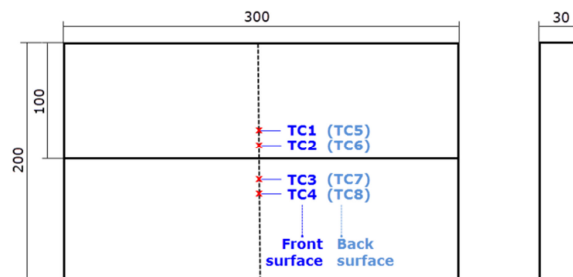


Figure 1. Dimensions of the RPEB weld (30-mm thick specimen) and thermocouple locations.

Welding Process

The welds were produced by TWI Cambridge, UK and were witnessed by University of Manchester staff. The plates were welded in the 2G-position, as shown in Figure 2, in a reduced-pressure vacuum chamber. A voltage of 150 kV and a current of 90 mA were used. The pre-heating temperature was 100°C.

The experiment was repeated twice, thus producing two identical benchmark samples. The reason for producing the second weld was to produce d0 specimens for subsequent neutron diffraction (ND) residual stress measurements. It also allowed the consistency of the welding procedure to be confirmed.

Instrumentation

The welded plates were instrumented with thermocouples (TC) to acquire the thermal transients induced due to the RPEB process. The thermocouple arrays were proposed based on numerical analysis. The array consisted of 8 TCs: four on the front surface (Figure 2a) and four on the back surface (Figure 2b). In each surface the TCs were placed symmetrically, at distances of 7mm and 15mm from the centreline of the weld. TC measurements are essential in order to validate the finite element thermal transient predictions. The sampling rate was 10 Hz.

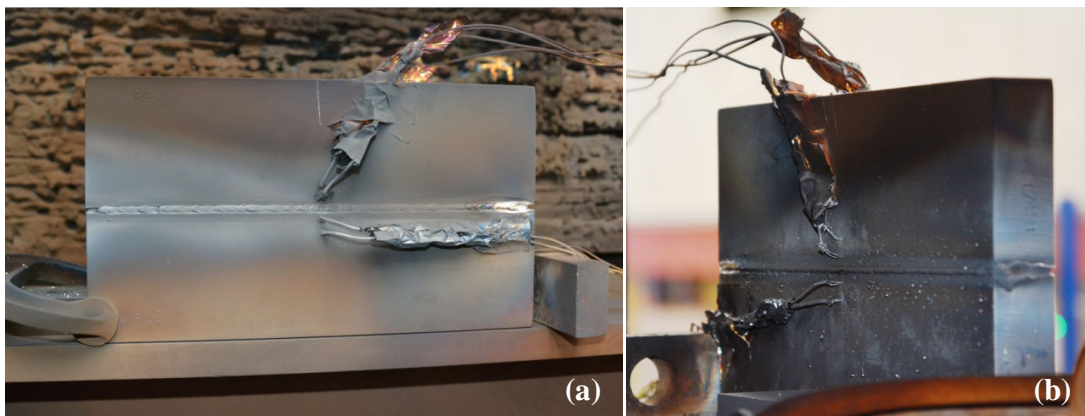


Figure 2. RPEB 30-mm thick single-pass weld specimen instrumented with thermocouples, after welding: (a) front surface; and (b) back surface.

Macrograph and Non-Destructive Evaluation of RPEB welds

The welds were radiographed to demonstrate that they were free of significant defects, according to the acceptance criteria in ASME IX:2013. A typical weld macrograph is shown in Figure 3.

Neutron Diffraction Measurements

For the Neutron diffraction (ND) experiment, a time of flight neutron source at UK-ISIS facility was employed to measure the residual stresses in longitudinal (L), transverse (T) and normal (N) directions. In the Engin-X instrument, two strain components were measured at once and the third component was measured by rotating the weld specimen by 90°. A nominal gauge volume of 3x3x3 mm was used for the measurement of longitudinal strains and 3x3x10 mm for the transverse and normal strain components. For d₀ measurements, a 5 mm thick stress-free comb was machined using EDM to measure the strain components in the same measurement grid adopted for the weld.

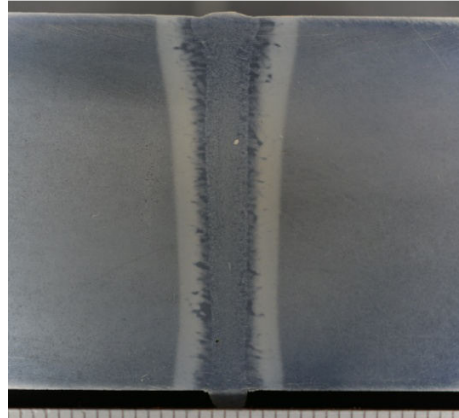


Figure 3. Macrograph of the RPEB 30 mm weld.

The strains acting in three directions $\epsilon_{L, T, N(x,y)}$ were calculated using the following expression

$$\epsilon_{L,T,N(x,y)} = \frac{d_{L,T,N(x,y)} - d_o(x,y)}{d_o(x,y)} \quad (2)$$

Similarly, the stresses acting in three directions $\sigma_{L, T, N(x,y)}$ were calculated using a generalised expression based on Hooks law, namely

$$\sigma_{L(x,y)} = \frac{E_{\{211\}}}{1+\nu_{\{211\}}} \left[\epsilon_{L(x,y)} + \frac{\nu_{\{211\}}}{1-2\nu_{\{211\}}} (\epsilon_{L(x,y)} + \epsilon_{T(x,y)} + \epsilon_{N(x,y)}) \right] \quad (3)$$

where $E_{\{211\}}$ and $\nu_{\{211\}}$ are the elastic modulus and Poisson's ratio, taken to be 216 GPa and 0.27, respectively (Daymond and Priesmeyer (2002)).

MODELLING AND SIMULATION

The welding simulation results of interest for this study are the residual stress fields developed during the RPEB welding process. These stresses are expected to be strongly affected by SSPT kinetics, which in turn is strongly affected by both the peak temperatures achieved and the heating/cooling rates achieved in the weld fusion zone and heat affected zone (HAZ). An accurate thermal transient solution is thus a prerequisite for an accurate residual stress prediction. A sequentially-coupled thermo-mechanical approach was followed, which is shown in previous work Venkata and Truman (2013) and Bendeich et al. (2012) as an accurate and computationally efficient methodology.

By explicitly accounting for thermo-metallurgical phenomena in a finite element (FE) model, numerical solutions are acquired at an increased computational cost. Preliminary analyses aimed to optimise the solution by performing mesh sensitivity studies. Because welding was performed in the 2G position, with the specimen bottom surface in contact with a large steel plate and the other surfaces radiating to vacuum, further studies examined the impact of neglecting this asymmetry and analysing a symmetric half-model rather than a full model.

The modelling and simulation procedure as well as the software employed are summarised below:

Step 1: FE geometry, mesh and preliminary model creation were performed using ABAQUS[®]/CAE version 6.13 (2013). The final model contained 25,000 elements. Since the phenomena to be

simulated are rapid, complex, and confined to a narrow region, the model was created with a sufficiently fine mesh in the weld bead and HAZ regions.

- Step 2: Heat source calibration was performed using the FEAT-WMT[®] software package (Smith (2013)). FEAT-WMT uses the welding parameters defined in Table 2 as an input to provide the appropriate volumetric power densities for the model. The thermal solution at this step was validated with TC measurements (Figures 1 and 2) and the fusion boundary shape (Figure 3).
- Step 3: Thermal FE analysis was performed using ABAQUS[®]/Standard. The thermal FE model was developed using DC3D20 elements. Both welding and cooling steps were simulated. A DFLUX subroutine was used to read the time-resolved volumetric power densities supplied by FEAT-WMT (Step 2) into the model. The thermal transients were again validated against the TC measurements.
- Step 4: Mechanical FE analysis was performed using ABAQUS[®]/Standard. This analysis used the temperature distribution calculated during Step 3 as an input. C3D20RH elements were used. The boundary conditions included the effect of gravity and the prevention of rigid body motion. A subroutine developed at the Australian Nuclear Science and Technology Organisation (ANSTO) was used to explicitly predict anisothermal SSPT phenomena (Hamelin et al. (2014)). The results were validated against the ND WRS measurements.

The thermo-physical and thermo-mechanical material properties used were temperature-dependent data from the recent work of Hamelin et al. (2014).

Cases Examined

The objective of the current study was to reveal the importance of transformation plasticity for single-pass, autogenous RPEB welding of 30-mm thick ferritic steel plates; for that reason three cases were examined, which are summarised in Table 3.

Table 3: Cases examined.

Case #	Abbreviation	Description
Case 1	“SSPT+TP”	Using a Solid-State Phase Transformation (SSPT) subroutine with Transformation Plasticity (TP). The subroutine was developed at the Australian Nuclear Science and Technology Organisation (ANSTO) and was used with the parameters proposed by the NeT-TG5 work of Hamelin et al. (2014).
Case 2	“SSPT-TP”	Model similar Case 1, using the same base subroutine, but excluding transformation plasticity phenomena.
Case 3	“noSSPT”	A simple mechanical FE model that does not explicitly account for any SSPT phenomena. Since the mean thermal expansion data implicitly captures isothermal SSPT phenomena, the influence of volumetric shape changes are considered (but not TP).

The three cases selected were considered to be indicative, to reveal the effect of transformation plasticity. Case 1 has been previously validated (Hamelin et al. (2014)) on the same ferritic steel, in the case of a single-pass autogenous GTAW edge beam weld. This case was considered to be a relatively complete approach for modelling the welding of ferritic steels, incorporating thermo-metallurgical effects combined

with TP. Case 2 is also examined, since the effect of TP has not been extensively studied on an EB weld and its effect – at least on modelling – might be counter-acted by other phenomena. Case 3 is used as a reference, to demonstrate the significance of taking into account anisothermal SSPT kinetics with TP.

RESULTS

The results of the investigation for all three cases are presented in the form of WRS contour plots (Figure 4) as well as in the form of WRS line plots (Figure 5) taken 12.5 mm below the upper surface of the specimen.

In Figure 4, the contour results of all three WRS components at the weld mid-length are considered, as denoted by a plane with red-coloured boundaries in Figure 4a. Each of the Figures 4b, 4c and 4d contain a direct comparison of the three cases examined (SSPT+TP, SSPT-TP, noSSPT) for each stress component (S33, S22 and S11, respectively). The contour range used is the same for all cases.

The weld fusion zone can be clearly recognised in Figure 4, for the cases where anisothermal SSPT kinetics are considered, by a very narrow region of high compressive stresses. When only isothermal SSPT kinetics are implicitly considered (Case 3), the tensile WRS from the HAZ extends into the fusion zone, such that these regions are indistinguishable from each other. In all cases, peak longitudinal stresses above 200 MPa are predicted in the HAZ; however, the tensile stress distributions just outside the HAZ are slightly different. The distribution appears to be smoother in the SSPT+TP case, whereas the variation of longitudinal stresses is more intense in the case of SSPT-TP model, as stresses rapidly vary from highly negative to highly positive over a narrow region of the fusion zone and HAZ.

Normal stresses are almost zero everywhere apart from the centre of the weld bead. Transverse stresses develop in a similar pattern as the longitudinal ones.

In Figure 5, the predicted outcomes are then compared with the ND-measured WRS. The ND measurement points belong to the line shown in Figure 4a, which is lying on the mid-length of the sample, at a distance of 12.5 mm from the top surface. Since the simulation results are obtained from a half model to take advantage of process symmetry, the experimental measurements from Side B (Figure 4a) were mirrored and plotted together with the measurements from Side A (squares in Figure 5).

Focusing on the experimental RS measurements, compressive stresses are measured for all stress components in the weld fusion zone; the largest compressive stresses are measured along the normal direction (over 500 MPa), followed by the longitudinal (over 150 MPa) and transverse (~130 MPa) stress components. These stresses acquire their minimum value at the centreline of the weld and then begin to rapidly increase until they reach their peak tensile value just outside the heat affected zone (HAZ). Moving further away from the weld bead and HAZ, these values fall to near-zero values. Note that in the case of transverse stress measurements, the experimental data is scattered.

Longitudinal WRS (Figure 5a) follow the so-called “M-shaped” profile, also observed in Kundu et al. (2013). This behaviour is expected for RPEB welds of ferritic steels, due to the influence of SSPT phenomena in the weld fusion zone and HAZ. WRS predictions from Cases 1 and 2 follow the stress distribution trend. The sign reversal in the stress values occurs near the locations indicated by the ND measurements: from compressive to tensile at 3 mm from the centreline and from tensile back to slightly compressive at 18.8 mm from the centreline. The predicted far-field stresses are approximate to the average from the two symmetrical measurements - in all cases, within the ND measurement error of ± 50 MPa.

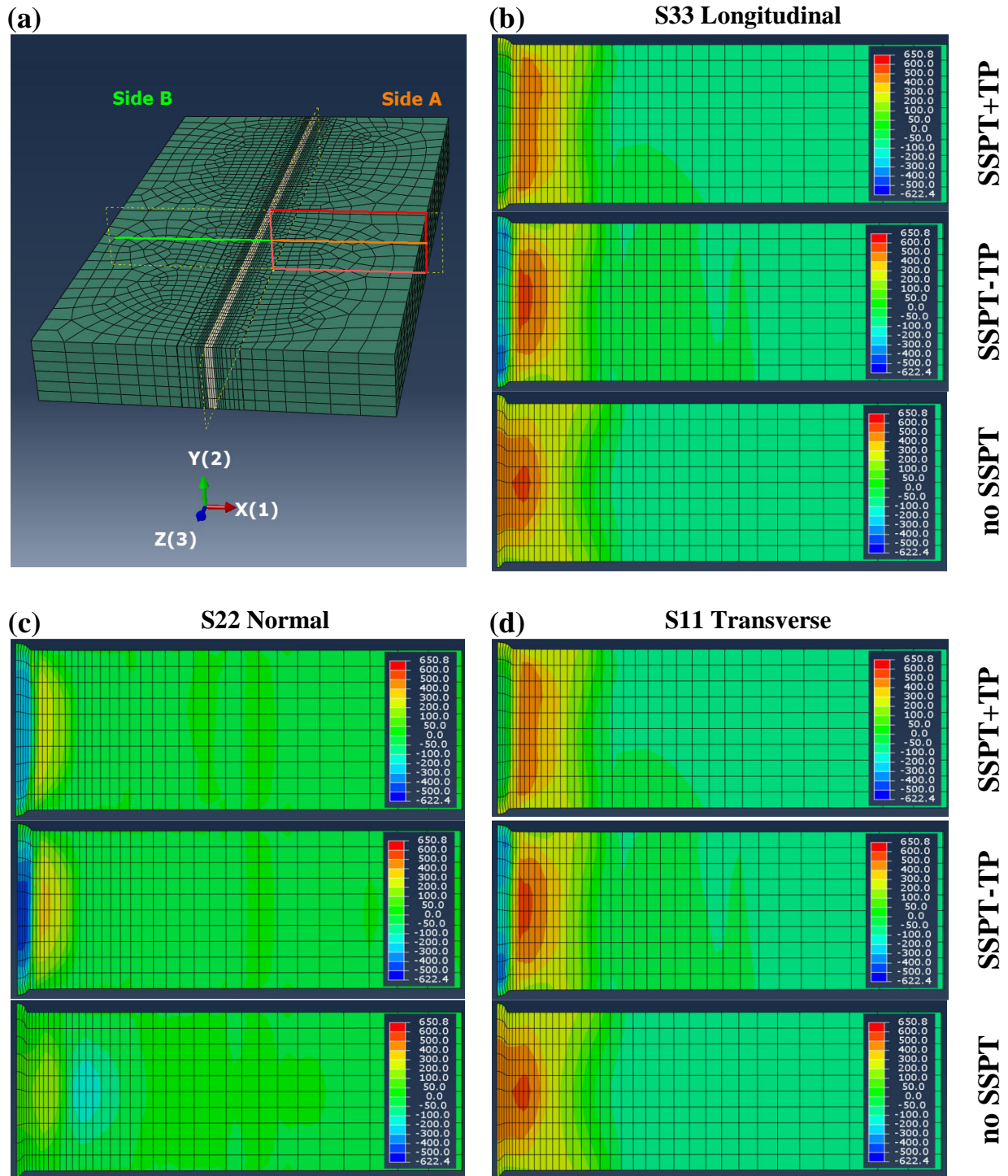


Figure 4. Predicted WRS components using the three cases outlined in Table 3, for (a) the half-model geometry shown: (b) longitudinal WRS; (c) normal WRS; and (d) transverse WRS.

The model that seems to be capturing the ND measurements the best is Case 2 (SSPT-TP). Peak longitudinal compressive stresses differ from measurements by an absolute error of 7.36 MPa (4.4%). Quantification of the main differences between the three models is summarised in Table 4. The SSPT+TP

model under-predicts the longitudinal compressive stresses in the weld bead, but still captures the peak tensile stresses quite well. Case 3 results confirm that the implicit consideration of isothermal SSPT kinetics is insufficient for accurate WRS predictions in the weld fusion zone. Different modelling approaches concerning TP also seem to have a significant effect on the predicted WRS.

Table 4: Absolute values of measured and predicted longitudinal stresses at the weld mid-length. Absolute and relative errors of the three models are shown.

Values at centreline	ND measurement	SSPT+TP	SSPT-TP	noSSPT
S33 absolute value	-166.25 MPa	-2.32 MPa	-158.889 MPa	+485.47 MPa
S33 absolute error	-	163.94 MPa	7.36 MPa	319.22 MPa
S33 relative error	-	98.6%	4.4%	192.0%

DISCUSSION

Comparison of measured and predicted WRS distributions has validated the assumption that anisothermal SSPT kinetics must be considered should the analyst wish an accurate weld simulation. By explicitly considering these kinetics using the subroutine developed by Hamelin et al. (2014), the analyst may also examine the post-weld ferritic phase distribution across the weld. This assessment is valuable in that it provides an additional level of model validation, and can also alert the analyst to any undesirable phases in the weldment (e.g. large amounts of martensite may significantly reduce weld toughness). While predicted phase distributions have been captured in this study, further discussion of these results lie outside the scope of this paper.

Based on the previous work of Hamelin et al. (2014), the most accurate WRS predictions were expected in the Case 1 solution, when TP is considered. However, the WRS comparison shown in Table 4 indicates that the Case 2 solution is more accurate. Since good agreement exists in the repeated ND measurements (i.e. along Sides A and B) of longitudinal WRS (Figure 5a), one can assume that the most likely source of error exists in the numerical model used for Case 1 predictions.

An examination of the subroutine developed to capture SSPT+TP has revealed a source of error in TP calculation that relates to the level of constraint present in the weld fusion zone. The SSPT subroutine captures TP both on heating as well as on cooling; based on the model of Greenwood and Johnson (1965), TP on heating is expected since strain compatibility is required as the material contracts during ferrite-austenite transition. Within the weld fusion zone, this TP will be removed from the material once the melting temperature has been exceeded; however, this relaxation had not been accounted for in the Case 1 model. As a result, these model results include a significant amount of compressive plastic strain in the weld fusion zone, which has been incorrectly kept in the material after melting. This invalid assumption had not been previously observed in validation studies (i.e. NeT TG5), since the constraint of the edge beam weld was not sufficient enough to create significant compressive TP upon heating.

To address this discrepancy, the SSPT subroutine has been modified to remove any accumulated TP once the melting temperature of the material is exceeded. RPEB simulations of the 30-mm thick specimen are currently underway using this revised subroutine; it is expected that higher compressive WRS will be predicted for all stress components using this model, due to the larger tensile plastic strains that will accumulate on cooling.

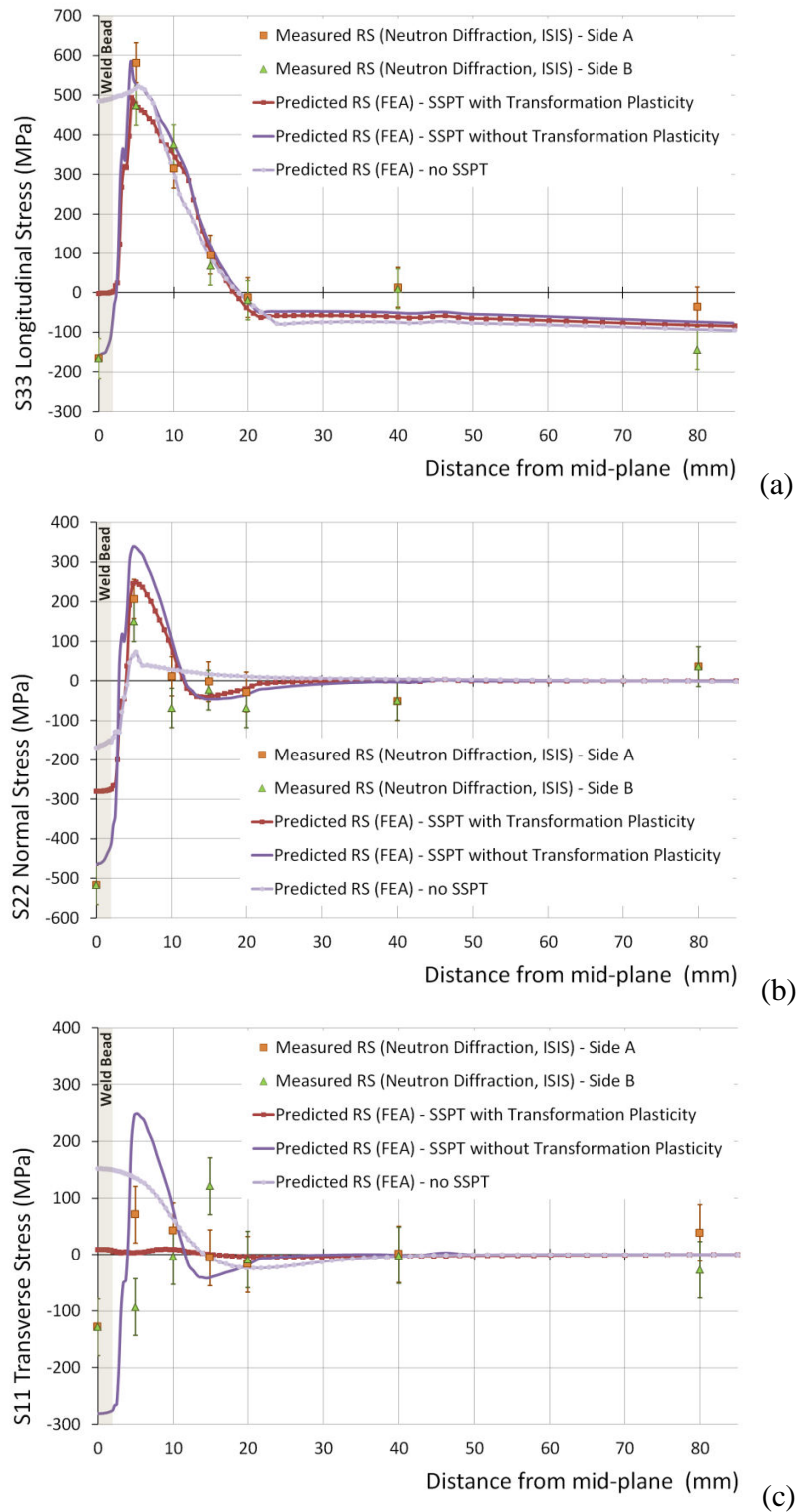


Figure 5. Line profiles of measured and predicted WRS, taken 12.5 mm below the upper surface of the weld: (a) longitudinal WRS; (b) normal WRS; and (c) transverse WRS.

CONCLUSIONS

Reduced pressure electron beam (RPEB) welding was numerically simulated using three different models: one model captured anisothermal SSPT kinetics including transformation plasticity (TP); one model captured anisothermal SSPT kinetics, without TP; and one model implicitly captured isothermal SSPT kinetics from the material data set used. The resulting stress distributions were compared with experimental weld residual stress (WRS) measurements using the neutron diffraction technique. Comparison of measured and predicted WRS reveal the models that consider anisothermal SSPT kinetics achieve better agreement with the experimental data, relative to models that consider isothermal kinetics. Transformation Plasticity (TP) has a significant impact on the stresses in the fusion zone; while the model that does not consider TP more accurately predicts the longitudinal WRS distribution, it over-predicts the compressive transverse WRS in the fusion zone. An invalid assumption in the SSPT subroutine was identified and removed, which will improve the accuracy of future model predictions.

ACKNOWLEDGMENTS

This research consists part of the EPSRC funded New Nuclear MANufacturing (NNUMAN) Program. The authors would like to thank the Manufacturing Technology Research Laboratory (MTRL) staff Mr Ian Winstanley and Mr Paul English; Dr Ondrej Muránsky from ANSTO; Dr Arben Ferhati, Mr Mike Nunn and Mr Kyle Power, TWI, Cambridge, UK for the collaboration and implementation of RPEB welds. The authors gratefully acknowledge the award of beam time at the Diamond Light Source.

REFERENCES

- Bendeich, Philip J., Ondrej Muránsky, Cory J. Hamelin, M.C. Smith, and Lyndon Edwards. (2012). "The Impact of Axi-Symmetric Boundary Conditions on Predicted Residual Stress and Shrinkage in a PWR Nozzle Dissimilar Metal Weld", *Proceedings of the ASME 2012 Pressure Vessels & Piping Conference PVP2012*. Toronto, Ontario, Canada.
- Daussault Systemes. (2013). "SIMULIA. ABAQUS/Standard."
- Daymond, M. R., and H. G. Priesmeyer. (2002). "Elastoplastic Deformation of Ferritic Steel and Cementite Studied by Neutron Diffraction and Self-Consistent Modelling." *Acta Materialia* 50 (6).
- Duffy, Christopher J. 2014. "Modelling the Electron Beam Welding of Nuclear Reactor Pressure Vessel Steel." University of Cambridge.
- Francis, J. A., H. K. D. H. Bhadeshia, and P. J. Withers. (2007). "Welding Residual Stresses in Ferritic Power Plant Steels", *Materials Science and Technology* 23 (9): 1009–20.
- Greenwood, G.W., and R.H. Johnson. (1965). "The Deformation of Metals under Small Stresses during Phase Transformations", *Proceedings of the Royal Society of London, Series A*, 283–403.
- Hamelin, Cory J., Ondrej Muránsky, Michael C. Smith, Thomas M. Holden, Vladimir Luzin, Philip J. Bendeich, and Lyndon Edwards. (2014). "Validation of a Numerical Model Used to Predict Phase Distribution and Residual Stress in Ferritic Steel Weldments", *Acta Materialia* 75: 1–19.
- Kundu, A, P J Bouchard, S Kumar, K a Venkata, J A Francis, A Paradowska, G K Dey, and C E Truman. (2013). "Residual Stresses in P91 Steel Electron Beam Welds", *Science and Technology of Welding & Joining* 18 (1): 70–75.
- Magee, C.L. (1966). "Transformation Kinetics, Microplasticity and Aging of Martensite in Fe-31Ni." *Pittsburgh, PA: Carnegie Institute of Technology*, p. 227.
- Sjöström, S. 1985. "Interactions and Constitutive Models for Calculating Quench Stresses in Steel." *Materials Science and Technology* 1 (10): 823–29.
- Smith, R.M. 2013. *FEAT-WMT: Weld-Modelling Tool User Guide*. Edited by FEATPLUS LIMITED. Bristol, UK: FeatPlus Limited.
- Venkata, K.A., and Christopher E Truman. (2013). "Finite Element Simulation of Laser Welding in a P91 Steel Plate", *Proceedings of the ASME PVP2013 Pressure Vessels and Piping Conference*, France.